A MATHEMATICAL MODEL FOR THE MOTION OF MECHANORECEPTOR HAIRS IN FLUID ENVIRONMENTS

BOB L. HENSON, *Department of Physics*
LON A. WILKENS, *Department of Biology, University of Missouri–St. Louis, St. Louis, Missouri 63121 U.S.A.*

ABSTRACT A differential equation has been derived for the motion of the mechanosensory hairs of animals when they are stimulated by the motion of their fluid environment. Specific solutions of the equation are obtained for three states of fluid flow including steady-state sinusoidal oscillations. The model is specifically applied to crayfish sensilla in an aqueous medium, but the assumptions of the model are also shown to be valid in air for the sensory hairs of insects. The calculations are consistent with available experimental data.

INTRODUCTION

The abdomen and thorax of the crayfish have numerous cuticular hairlike mechanoreceptors on their surfaces. Experiments have shown that various mechanosensitive interneurones respond to hair sensilla motion induced by water environment disturbances (Wilkens and Larimer, 1972; Wiese. et al., 1976; Flood and Wilkens, 1978). However, conclusions regarding response magnitude and directional sensitivity of these interneurones have been based largely on qualitative evidence concerning the receptor displacements mediated by the water currents.

The purpose of this study is to provide a quantitative description of mechanoreceptor hair movements for given states of fluid motion. The mathematical model developed here refers specifically to mechanoreceptors of the southern crayfish *Procambarus clarki*, which have been the subject of a recent study by Wiese (1976). However, the model is sufficiently general so as to be applicable to any type of hair sensilla that responds to the motion of its fluid environment. This model should also be applicable to the motion of receptors in air, e.g., the filiform hairs of cricket cerci (Dumpert and Gnatzy, 1977) and the thoracic hairs of caterpillars (Tautz, 1977).

THE MODEL

Our model consists of three compartments. The fluid serves as one compartment, with the hair and the attachment surface forming the second and third compartments, respectively. In developing the mathematical model we derive a differential equation for the angular displacement of the hair, as a function of time, by considering the fluid-hair interaction forces together with the hair-surface interaction forces. The equation is derived for arbitrary fluid displacements, although solutions are obtained specifically for three types of fluid motion including sinusoidal oscillations.

Assumptions

For equilibrium conditions we assume that the hair is perpendicular to the surface with no fluid motion. While this assumption simplifies our calculations it does not restrict the model, as other equilibrium conditions can be obtained by simple coordinate transformations. Upright hairs are perpendicular to the exoskeletal surface in most cases (Mellon; 1963; Wiese, 1976). Calculations are for hair motions in the vertical plane under one-dimensional laminar fluid flow conditions; that is, we assume that the fluid flow is parallel to the plane surface to which the hair is attached. It is further assumed that the hair-fluid coupling interactions are due to viscous forces on uniform cylindrical hairs, and that the hairs reside completely within the thin laminar boundary-layer of nominal thickness, δ, near the surface. Under these conditions, the fluid velocity distribution in the boundary-layer region of interest varies quadratically with height, y, above the surface and is given by $V(t)[(2y/\delta) - (y^2/\delta^2)]$ where $V(t)$ is the magnitude of the fluid velocity outside the boundary-layer. Rouse (1938) has shown this to be a good approximation for thin boundary-layers. While the hairs are usually somewhat cone-shaped, an average effective radius can be used that will compensate for the uniform cylinder assumption. The equations for viscous forces on cone-shaped hairs do not seem to be mathematically tractable.

We have also assumed that hair stiffness restricts bending to the hinge region at the surface of the animal. Furthermore, for small angular displacements of the hair, it is reasonable for the restoring torque on the hair at the hinge to be proportional to the angular displacement. That, we expect this restoring torque to obey a Hooke's law-type equation. We also include a damping torque on the hair due to dissipative processes in the hinge. This torque is proportional to the angular velocity of the hair.

Since the hair is short and of small diameter it is likely that the hair does not overtly disturb the laminar flow of the fluid. Also, gravitational effects on the hair as well as edge effects near the end of the hair are negligible.

Derivation

In the derivation we use a coordinate system with the origin at the hair's hinge. The abscissa is parallel to the direction of the fluid flow and the ordinate is perpendicular to the surface. Fig. 1 is a diagram of the coordinate system depicting the various force and velocity vectors. Theta (θ) represents the angle between the hair and the positive y axis where $\theta > 0$ for a rotation of the hair toward the positive direction of the x axis. The distance from the hinge to a point on the hair will be designated by r. We let dF be the component of the viscous force that is

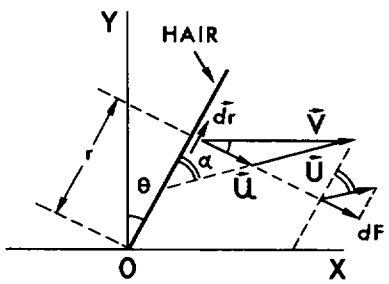

FIGURE 1 Coordinate system and vector diagram used in the derivation.

exerted perpendicular to the hair on an elemental length dr of the hair. Then dF will be approximately proportional to the component of the velocity of the fluid relative to the hair, that is, perpendicular to the axis of the hair. We let α be the angle between **dr** and U, where $\mathbf{U} = \mathbf{v} - \mathbf{u}$ is the velocity of the fluid relative to the hair. Here **v** and **u** are, respectively, the velocities of the fluid and the hair at dr measured with respect to the coordinate system.

Lamb (1932) has shown that under conditions of a low Reynolds number, the force per unit length on a cylinder, due to the component of the relative velocity perpendicular to the cylinder axis, is

$$\frac{dF}{dr} = \frac{4\pi\eta U \sin\alpha}{0.5 - \gamma - \ln\left(\dfrac{\rho R^2 U \sin\alpha}{2\eta}\right)} \equiv kU \sin\alpha, \tag{1}$$

where $\gamma \approx 0.58$, R is the radius of the cylinder, ρ is the density of the fluid, and η is the dynamic fluid viscosity coefficient. The log term is slowly varying and thus can be treated as nearly constant compared to the numerator for small changes in $U \sin\alpha$, which means the parameter k is essentially a constant.

The force dF from Eq. 1 causes a torque $d\tau = r\,dF$ on the hair. Rewriting Eq. 1 as $dF = k|\mathbf{U} \times \mathbf{dr}|$ with U and **dr** expressed in our coordinate system and then integrating with respect to r, we obtain for the magnitude of the torque due to the fluid-hair interaction

$$\tau = \left[\frac{2V(t)}{\delta}\cos^2\theta - \frac{3V(t)L}{4\delta^2}\cos^3\theta - \dot{\theta}\right]\frac{kL^3}{3}, \tag{2}$$

where L is the hair length and $\dot{\theta}$ is the time derivative of θ.

If we assume a restoring torque of $-K\theta$ and set the net torque equal to the product of the effective moment of inertia I of the hair and $\ddot{\theta}$, we obtain the differential equation

$$I\ddot{\theta} + \left(\beta + \frac{kL^3}{3}\right)\dot{\theta} + K\theta = V(t)\left[\frac{2\cos^2\theta}{\delta} - \frac{3L\cos^3\theta}{4\delta^2}\right]\frac{kL^3}{3}. \tag{3}$$

The quantity $-\beta\dot{\theta}$ is the damping torque due to dissipative processes in the hair hinge. Although β may be small in many cases, we have included it for completeness. The parameters β and K for the hair hinge are assumed to be nearly constant.

Since Eq. 3 is nonlinear and is not generally tractable, we use the small angle approximation $\cos\theta \approx 1$, which linearizes it. In our applications the hair displacement angle is observed to be much less than 10° and hence this approximation is a very good one. After linearization Eq. 3 reduces to

$$I\ddot{\theta} + \left(\beta + \frac{kL^3}{3}\right)\dot{\theta} + K\theta \approx V(t)\left[\frac{2}{\delta} - \frac{3L}{4\delta^2}\right]\frac{kL^3}{3}. \tag{4}$$

Eq. 4 is an example of a damped, forced oscillator-type differential equation and can be reduced to quadratures. Hereafter we will use

$$\mu(t) \equiv V(t)\left[\frac{2}{\delta} - \frac{3L}{4\delta^2}\right] \tag{5}$$

for convenience in writing our equations.

Steady-State Sinusoidal Fluid Motion

For sinusoidal variations of $V(t)$ the solutions are readily available (e.g., Symon, 1960) so only the results will be quoted here. This case is of interest since waves in shallow water cause nearly sinusoidal water displacements near the bottom and provide stimuli for crustaceans. The sinusoidal steady-state solution shows that the hair amplitude θ_0 is

$$\theta_0 = \frac{kL^3}{3}\mu_0\left[(K - I\omega^2)^2 + \omega^2\left(\beta + \frac{kL^3}{3}\right)^2\right]^{-1/2} \tag{6}$$

and the phase angle of the hair position with respect to the phase of the fluid velocity is

$$\phi = -\arctan\left[\frac{\omega\left(\beta + \frac{kL^3}{3}\right)}{K - I\omega^2}\right]. \tag{7}$$

Here $\omega/2\pi \equiv f$ is the frequency of oscillation, and μ_0 is the amplitude of $\mu(t)$.

Linear Time-Dependent Fluid Motion

For this particular type of fluid motion, $\mu(t) = \mu_1 t + \mu_0$, where μ_1 and μ_0 are constants. Eq. 4 then becomes

$$I\ddot{\theta} + \left(\beta + \frac{kL^3}{3}\right)\dot{\theta} + K\theta \approx \frac{kL^3}{3}(\mu_1 t + \mu_0). \tag{8}$$

It should be pointed out that in this case we have assumed there is an impulsive increase in fluid velocity at $t = 0+$, which results in the term given by μ_0. In addition to this stepwise increase in velocity at $t = 0+$ there is a uniform acceleration of the fluid for $t \geq 0$, which results in $\mu_1 t$. We assume that for $t \leq 0$ the fluid is at rest.

Eq. 8 can best be solved by using the technique of Laplace transforms. By assuming that the hair is at rest and vertical at $t = 0$, the Laplace transform of Eq. 8, after rearranging terms, is

$$\Psi(s) = \frac{kL^3}{3}\left[\frac{\mu_1}{s^2} + \frac{\mu_0}{s}\right]\left[\left((s + b)^2 + \left(\frac{K}{I} - b^2\right)\right]^{-1}, \tag{9}$$

where $\Psi(s)$ is the Laplace transform of $\theta(t)$ and

$$b \equiv \frac{1}{2I}\left(\beta + \frac{kL^3}{3}\right). \tag{10}$$

For convenience we let

$$a^2 \equiv \frac{K}{I} - b^2. \tag{11}$$

There are three possible solutions for Eq. 9 depending on the range of values of a^2. To obtain solutions we take the inverse Laplace transform of Eq. 9 to get

$$\theta(t) = \frac{kL^3\mu_1}{3Ia}\int_0^t \exp[-bu]\sin(au)(t-u)\,du + \frac{kL^3\mu_0}{3Ia}\int_0^t \exp[-bu]\sin(au)du. \tag{12}$$

The integrals in Eq. 12 are tractable, but the results are rather long. For $a^2 > 0$ the result is a superposition of damped, sinusoidal oscillations with an asymptotic solution. This condition can occur for relatively large hair masses and large values of K with weak viscous coupling between the fluid and the hair. This case is most likely to be relevant for insects in air. The characteristic time-constant for the decaying oscillations is

$$b^{-1} = \frac{6I}{3\beta + kL^3} \tag{13}$$

and the frequency f of these oscillations is given by

$$f = \frac{a}{2\pi} = \frac{1}{2\pi}\left[\frac{K}{I} - b^2\right]^{1/2}. \tag{14}$$

Since we are primarily interested in the asymptotic solution, it can be obtained from Eq. 12 by letting $t \to \infty$ in the limits of the integrals and evaluating the resulting definite integrals. After substituting for a and b this yields

$$\theta(t) \approx \frac{kL^3}{3K}\left[\mu_1 t + \mu_0 - \frac{\mu_1}{K}\left(\beta + \frac{kL^3}{3}\right)\right]. \tag{15}$$

This asymptotic solution is only valid for times such that $t \gg 6I/(3\beta + kL^3)$, but since we expect I to be very small, this should not be unduly restrictive. That is, we expect the oscillations given by Eq. 15 to damp out rather rapidly in our applications. In applications where β is negligibly small, this time-constant will vary inversely with the hair length, since $I \propto L^2$. It should be pointed out that the asymptotic solution given by Eq. 15 is in fact independent of the effective moment of inertia I of the hair.

The second solution of Eq. 9 is for $a^2 < 0$ and it represents an overdamped motion of the hair. This solution occurs for relatively small hair masses and small values of K with strong fluid-hair coupling forces. This case is most apt to be applicable to crustaceans in water. This solution can be obtained from Eq. 12 by replacing the constant a with $i[b^2 - \mathrm{K}/I]^{1/2} = ia'$, where $i = \sqrt{-1}$. This solution consists of a superposition of purely exponential-type decaying terms with an asymptotic solution. Two time-constants are involved, $(b + a')^{-1}$ and $(b - a')^{-1}$. Here there are no oscillations, but the transient effects decay comparatively slowly because $b - a'$ can be a rather small number. That is, the terms with the time-constant $(b + a')^{-1}$ decay rather rapidly, but the terms involving the time-constant $(b - a')^{-1}$ decay comparatively slowly. The solution that remains after the transient terms vanish is the same as that for $a^2 > 0$ and is given by Eq. 15.

In the overdamped case, β is likely to have a negligible effect on the hair motion in an aquatic medium because of the relatively strong fluid-hair coupling. However, this is not likely to be true in air.

The third solution for Eq. 9 represents a critically damped type motion for the hair. This

solution is obtained by taking the inverse Laplace transform of Eq. 9 after setting $a^2 = K/I - b^2 = 0$. The complete solution is

$$\theta(t) = \frac{kL^3\mu_1}{3I}\int_0^t ue^{-bu}(t-u)\,du + \frac{kL^3\mu_0}{3I}\int_0^t ue^{-bu}\,du, \tag{16}$$

for which the resulting asymptotic solution is

$$\theta(t) \approx \frac{kL^3}{3Ib^2}\left[\mu_1 t + \mu_0 - \frac{2\mu_1}{b}\right]. \tag{17}$$

The condition for critical damping of the hair may be an optimal one, physiologically, in the sense that for this condition the hair will return to its equilibrium position in minimum time after an initial displacement of the hair. The overdamped condition results in a mechanoreceptor hair that is sluggish. The underdamped condition, which causes decaying sinusoidal oscillations of the hair, may be of physiological importance in some frequency dependent applications in that it indicates a natural resonance frequency for the mechanoreceptor hair.

APPLICATIONS OF THE MODEL

Aquatic Medium

The validity of this model requires that the hair lie within the surface boundary-layer. Wiese (1976) reported typical hair lengths of $L \approx 500$ μm, with hair radii of $R \approx 7.5$ μm, for mechanoreceptors on the crayfish telson. It is known that the nominal boundary-layer thickness δ is the same order as the square root of the kinematic viscosity γ (Rouse, 1938). For water at 20°C, $\gamma \approx 10^{-2}$P cm^3 g^{-1}, which yields $\delta \sim 0.1$ cm. Thus, the hair length $L < \delta$, so that the hair is well within the boundary-layer and our model assumptions are valid here.

Numerical values of the various constants are needed to characterize the particular state of motion of the hair for either the transient or steady-state cases. Depending on these values, the hair motion will either be overdamped, critically damped, or underdamped. From Eq. 2 we calculate the water-hair coupling constant $k \approx 1.2 \times 10^{-2}$ dyn cm^{-2}s by using a typical value of $U = 1.0$ cm s^{-1}. We also obtain an approximate value for $\mu(t) = V(t)\,[(2/\delta) - (3L/4\delta^2)] \approx 16.25V(t)$ s^{-1}, using $\delta \approx 0.1$ cm and $L = 0.05$ cm. Also, Wiese (1976) has obtained torque-displacement data that enable us to compute the hair hinge spring constant to be $K \approx 1.22 \times 10^{-4}$ dyn cm. Although there does not seem to be any experimental data available to compute the damping constant β for the hair hinge, the model still predicts considerable information about the state of motion of the hair without knowing the precise value of β. In fact, as we argued earlier, β is probably negligible for applications in a water medium. From Eq. 11, with $a = 0$, we find that the value of b for critical damping is $b = \sqrt{K/I} \approx 1{,}210$ s^{-1} for an estimated moment of inertia of the hair $I \approx \frac{1}{3}\,mL^2 \approx 8.33 \times 10^{-11}$g cm^2 where m is the hair's mass. Since $(kL^2/6I) \approx 3{,}000$ s^{-1}, Eq. 10 shows that for any value of $\beta \geq 0$, $b > 1{,}210$ s^{-1}. Thus, for crayfish mechanoreceptor hairs in water the motion is always overdamped regardless of the β value.

By using these numerical constants, the equations for sinusoidal fluid motion (Eqs. 6 and 7) can be simplified by approximations at low frequencies. The amplitude θ_0 of the motion of the mechanoreceptor hair is $\theta_0 \approx (kL^3\mu_0/3K)\{1 - [(\beta + kL^3/3)^2/2K^2]\omega^2 + (I/K)\omega^2\}$ and the

phase angle is $\phi \approx -(\omega/K)[\beta + (kL^3/3)]$. If we assume that the amplitude of the far-field fluid velocity is $V_0 = 1.0$ cm s^{-1} we see that the amplitude is nearly constant $\theta_0 \approx 6.7 \times 10^{-2}$ rad for frequencies $\lesssim 6$ Hz. The phase angle of the hair relative to the phase angle of the fluid motion is directly proportional to the frequency for $f \lesssim 6$ Hz. At a frequency of 6 Hz the phase angle $\phi \approx -0.15$ rad; at 1.8 Hz, $\phi \approx -0.046$ rad, provided $\beta \ll k(L^3/3)$. For larger values of β the phase angle lags by a greater amount. Here it should be pointed out that Eq. 7 has two solutions and so far we have only given the one that is nearly in phase with the fluid motion at low frequencies.

Fig. 2 shows the amplitude θ_0 and phase angle ϕ as functions of the frequency f as plotted from Eqs. 6 and 7 for $\beta = 0$. Here we have plotted both solutions for ϕ. One solution shows a lagging phase angle, whereas the other one shows a leading phase angle. In most cases we believe that the negative solution is the relevant one. However, other small disturbances of the hair may cause the positive solution to be significant at times, so we have included it for completeness. The vertical dashed line represents the critical frequency at which the magnitude of the phase angle is 90°. This frequency is $f = \sqrt{K/I}/2\pi \approx 193$ Hz for the estimated value of I used here. Since this critical frequency depends on the value of I, it is possible that its measurement may be useful for obtaining empirical values of the effective

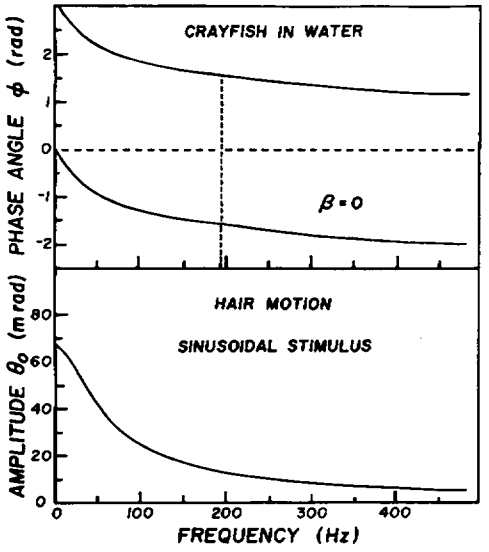

FIGURE 2

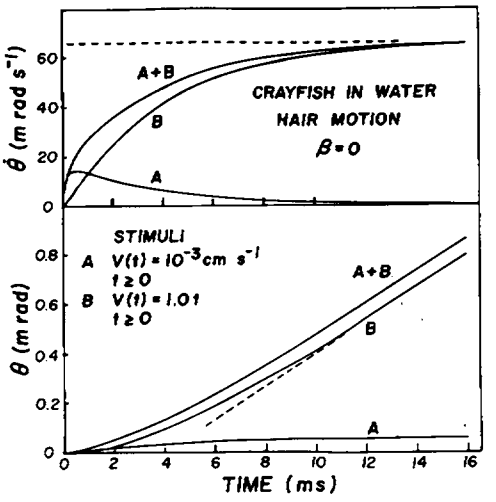

FIGURE 3

FIGURE 2 Theoretical steady-state response of a crayfish mechanoreceptor sensillum (500 μm long) to sinusoidal fluid motion. The amplitude of hair displacement (lower graph) and phase angle of the hair with respect to fluid velocity (upper graph) are plotted as a function of the stimulus frequency (for a maximum water velocity $V_0 = 1.0$ cm s^{-1}). The negative one of the two possible solutions for phase angle is expected to apply in most cases.

FIGURE 3 Predicted transient response of a crayfish mechanoreceptor (500 μm) to aperiodic fluid motion. Angular displacement θ (lower graph) and angular velocity $\dot{\theta}$ (upper graph) are plotted with respect to time. Curve *A* results from a stepwise water velocity increment at $t = 0$, whereas curve *B* results from a constant acceleration of the water. For these curves it has been assumed that the damping constant β is negligible.

moment of inertia for the hair. In the lower portion of Fig. 2, we observe that the amplitude drops off rapidly with frequency for $f \gtrsim 6$ Hz. For frequencies $f \gtrsim 200$ Hz, the amplitude becomes nearly proportinal to f^{-1}.

In Fig. 3, the predicted angular displacement θ and the angular velocity $\dot{\theta}$ have been plotted versus time for various transient stimuli using $\beta = 0$ with overdamped solutions. This figure shows the resulting mechanoreceptor motion for two states of motion of the fluid stimulus (A and B) along with a superposition of the two ($A + B$). That is, the predicted response of the hair is plotted for a fluid motion that accelerates uniformly (B) and for an impulsive steplike velocity change (A). It should be noted that a rather small step-wise impulsive change in fluid velocity (i.e., $\Delta V(t) = 10^{-3}$ cm s^{-1}) causes a relatively large response by the hair.

In Fig. 3 with $\beta = 0$, we see that steady state is reached at $t \gtrsim 15$ ms. If β is as large as 5×10^{-7}, asympotic conditions do not prevail until after $t \gtrsim 32$ ms. The overdamped transient motion results from two time-constants as we stated earlier. For crayfish, one of these $(b + a')^{-1}$ is of very short duration with times on the order of tenths of milliseconds, whereas the other one, $(b - a')^{-1}$, has typical values of tens of milliseconds. In general, these time-constants depend on L, but for mechanoreceptors where $\beta \ll k(L^3/3)$ both time-constants are independent of hair length for $L \gtrsim 318$ μm. For hair lengths $\lesssim 318$ μm, the motion is underdamped if $\beta = 0$. However, if $\beta \gtrsim 5 \times 10^{-8}$ dyn cm s, the motion is overdamped for all values of L.

Atmospheric Medium

In these applications, we find that there is insufficient experimental data to fully test the validity of our model. However, there is sufficient data for crickets and caterpillars to test the assumptions on which our model is based. For air at normal atmospheric pressure the kinematic viscosity coefficient at 25°C is $\gamma \approx 0.156$ P cm^3 g^{-1}. This yields a boundary-layer thickness of $\delta \sim 0.39$ cm. Tautz (1977) finds that the thoracical hairs on the caterpillars of *Barathra brassicae* have average lengths of 500 μm with average basal diameters of 5 μm. Dumpert and Gnatzy (1977) report that the lengths of the filiform hairs on the cerci of the cricket *Gryllus bimaculatus* vary from 30 μm to 3 mm. Thus, the mechanoreceptor hair lengths for both of these species are such that they are completely within the boundary-layer. Also, the hairs are of small diameter and nearly cylindrical. Thus, we see that the assumptions of our model are realistic for the mechanoreceptor hairs for these two species and data from them could be used to test our model.

It should be remarked that Tautz (1977) found evidence that enables us to conclude that the hinge damping constant β and the hinge spring constant K for thoracic hairs on the caterpillar are such that the hair motion is underdamped. That is, he observed rapidly damped oscillations of the hair when it was perturbed from equilibrium. This oscillation frequency could be used to determine the damping constant β if the hinge spring constant K were known. The spring constant K could be found from torque-angular displacement data for the hair, but sufficient information for the calculation is not available (Tautz, 1977).

SUMMARY AND CONCLUSIONS

We have obtained a differential equation for the mechanoreceptor hair motion in a fluid environment where the hair-fluid coupling is due to viscous forces. The assumptions for our

model appear to be physically realistic for the mechanosensory hairs on the tail surface of the crayfish, thoracic hairs of caterpillars, and filiform hairs of crickets. The only approximation that was used in the solution of the mathematical model was the assumption of small angles. The final solutions indicate that this small angle approximation is indeed valid and the results are consistent with qualitative and quantitative evidence from these three animals. Precise quantitative tests of the model will require further experimentation. This model is likely to be important and probably necessary for accurate interpretation of the responses of sensory cells to fluid motion stimuli.

This work has been supported in part by research grants from the National Institutes of Health (NS-12971-03) (to Dr. Wilkens) and the University of Missouri–St. Louis.

This paper is a contribution (No. 124) of the Tallahassee, Sopchoppy, and Gulf Coast Marine Biological Association.

Received for publication 26 December 1978 and in revised form 30 March 1979.

REFERENCES

DUMPERT, K., and W. GNATZY. 1977. Cricket combined mechanoreceptors and kicking response. *J. Comp. Physiol. A. Sens. Neural. Behav. Physiol.* **122**:9–25.

FLOOD, P. M., and L. A. WILKENS. 1978. Directional sensitivity in crayfish mechanoreceptive interneurons: analysis by root ablation. *J. Exp. Biol.* **77**:89–106.

LAMB, H. 1932. Hydrodynamics. Cambridge University Press, Cambridge. 1945, Dover ed. 614–616.

MELLON, D. 1963. Electrical responses from dually innervated tactile receptors on the thorax of the crayfish. *J. Exp. Biol.* **40**:137–148.

ROUSE, H. 1938. Fluid mechanics for hydraulic engineers. United Engineering Trustees, Inc., London. 1961, Dover ed. 195–200.

SYMON, K. R. 1960. Mechanics. Addison-Wesley Publishing Company, Inc., Reading, Mass. 50–52.

TAUTZ, J. 1977. Reception of medium vibration by thoracal hairs of caterpillars of *Barathra brassicae* L. *J. Comp. Physiol.* **118**:13–31.

WIESE, K. 1976. Mechanoreceptors for nearfield water displacements in crayfish. *J. Neurophysiol.* **39**:816–833.

WIESE, K., R. L. CALABRESE, and D. KENNEDY. 1976. Integration of directional mechanosensory input by crayfish interneurons. *J. Neurophysiol.* **39**:834–843.

WILKENS, L. A., and J. L. LARIMER. 1972. The CNS photoreceptor of crayfish: morphology and synaptic activity. *J. Comp. Physiol.* **80**:398–407.